Received: 11 January 2021 | Revised: 12 February 2021 | Accepted: 27 February 2021

DOI: 10.1002/aoc.6231

FULL PAPER

Applied Organometallic Chemistry WILEY

Structural elucidation, molecular modeling, and biological and antioxidant studies of phenanthroline/nicotinamide metals complexes

Walaa H. El-Shwiniy[1,2] | **Mohamed G. Abd Elwahed**[1] | **Reham M. Saeed**[1] | **Wael A. Zordok**[1,3] | **Sameh I. El-Desoky**[4]

[1]Department of Chemistry, Faculty of Science, Zagazig University, Zagazig, Egypt

[2]Department of Chemistry, College of Science, University of Bisha, Bisha, Saudi Arabia

[3]Department of Chemistry, University College of Quanfudha, Umm Al-Qura University, Al Qunfudhah, Saudi Arabia

[4]Regional Joint Laboratory, Directorate of Health Affairs, The Arab Republic of Egypt, Zagazig, Egypt

Correspondence
Walaa H. El-Shwiniy, Department of Chemistry, Faculty of Science, Zagazig University, Zagazig, 44519, Egypt.
Email: walaa1986@zu.edu.eg; whelmy@ub.edu.sa

Funding information
University of Bisha; Zagazig University

Three new cobalt (II), nickel (II), and copper (II) complexes [M (nicotinamide) (phenanthroline)$(H_2O)_3$]$Cl_2 \cdot 3H_2O$ (where M: Co (II), Ni (II) and Cu (II)) have been prepared and characterized by elemental analysis, Fourier transform infrared (FT-IR), and ultraviolet/visible (UV–Vis) spectroscopy as well as thermal analysis. The molar conductance measurements proved that the complexes were electrolytes. The results obtained from FT-IR confirm that the metal atoms were coordinated by one nitrogen atom from nicotinamide (NA) ligand, two nitrogen atoms from phenanthroline (Phen), and three oxygen atoms from three different water molecules. The complexes have octahedral structure. thermogravimetry (TGA) and its differential (DTG) analyses confirmed the suggested stereochemistry. Coats–Redfern and Horowitz–Metzger equations were used to calculate kinetic and thermodynamic parameters. Molecular modeling calculations confirm the structural geometry of the complexes, and the data indicate that the complexes are soft with respect to ligands where absolute softness (σ) varied from 5.34 to 13.33 eV, whereas σ for NA and Phen are 5.34 and 8.19 eV, respectively. The ligands and their complexes were assayed for their in vitro antimicrobial activities against some bacterial and fungal strains; the data showed that the complexes were active against some bacterial species compared with NA and Phen. Moreover, complexes and ligands revealed excellent antioxidant properties and could be useful in fighting the free radicals which occur in close connection with cancerous cells.

KEYWORDS

antioxidant, biological activity, modeling, phenanthroline/nicotinamide complexes, spectroscopy

1 | INTRODUCTION

Nicotinamide (NA) drug (also known as niacinamide) is the amide of nicotinic acid (vitamin B3/niacin) (Figure 1a). NA is a component of both vitamin B complex and co-enzyme, nicotinamide adenine dinucleotide (NAD). NA is considered as one of the important compounds that show both biological and coordinative characteristics.[1] NA itself plays an important role in the metabolism of living cells, and some of its metal complexes are biologically active as antibacterial or insulin-mimetic agents.[2] Therefore, the structure of NA

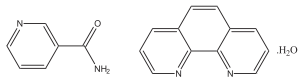

(a) (b)

FIGURE 1 The chemical structure of (a) nicotinamide (NA) and (b) 1,10-phenanthroline monohydrate (Phen)

has been the subject of many studies.[3,4] These pharmaceutical activities were extremely vital for the movement of hydrogen in cell respiration via NA. The NA structure is really the target of several experiments. NA is a pharmacologically and physiologically active reagent[2–7] since pyridine derivatives are associated with substantial biological function, such as fungicidal, antitumor, and antibacterial activities.

The heterocyclic organic compound phenanthroline (Phen) (Figure 1b) is a white solid which is soluble in organic solvents. It is used as a ligand in coordination chemistry, creating heavy complexes with the lot of metals. Phen is a bidentate ligand capable of coordinating metal sites by nitrogen atoms. Phen is a rigid ligand, with exception of bipyridine, where the pyridyl groups are joined together by an aromatic framework. Phen is similar to 2,2′-bipyridine (Bipy) in terms of their coordination properties but links metals more carefully since the donors of chelating nitrogen are preorganized. Phen is, however, a smaller donor than Bipy.[8,9]

In biological inorganic chemistry,[4,7–9] mixed-ligand chelates play a critical role. Metal-based antioxidants have recently gained recognition for their ability to support organisms and cells from oxidative stress-induced damage.[4] In the present research, various methods such as physico-chemical, spectroscopic (ultraviolet/visible [UV–Vis], Fourier transform infrared [FT-IR], ^{1}H NMR), and thermal analysis are used to prepare and structurally elucidate the transition metal complexes of a mixed ligand of NA and Phen. Density Functional Theory (DFT) is utilized to detect the exact configuration of the complexes and quantify total energy, formation heat, and total dipole moment. Also, the biological and antioxidant effectiveness has been checked.

2 | EXPERIMENTAL

2.1 | Materials and instruments

NA was purchased from the Western Pharmaceuticals Company. 1,10-Phenanthroline (99.90%) was obtained from Merck Chemical. $COCl_2{\cdot}6H_2O$ (99.90%), $CuCl_2{\cdot}2H_2O$ (99.90%), $NiCl_2$ (99.90%). Both solvents (99.90%) were imported from Fluka Chemical Company. The chemicals have been used as available with no purifying. The apparatus name and their models are summarized in Table 1.

2.2 | Synthesis of mixed ligand complexes

The pink solid complex $[Co(NA)(Phen)(H_2O)_3]Cl_2{\cdot}2H_2O$ was prepared by adding 1 mmol (0.238 g) of $CoCl_2{\cdot}6H_2O$ in 20 ml acetone drop-wise to a stirred suspended solution of 1 mmol (0.18 g) of 1,10-phenonathroline (Phen) with 1 mmol (0.35 g) NA in 50 ml acetone. The reaction mixture was refluxed for 8 h; the formed precipitate was filtered off, washed several times with acetone, and dried under vacuum over anhydrous $CaCl_2$. The pale blue and cyan solid complexes: $[Ni(NA)(Phen)(H_2O)_3]Cl_2{\cdot}H_2O$ and $[Cu(NA)(Phen)(H_2O)_3]Cl_2{\cdot}H_2O$, were prepared similarly at 1:1:1 molar ratio (M: NA: Phen) (Figure 2).

2.2.1 | $[co(NA)(Phen)(H_2O)_3]Cl_2{\cdot}2H_2O$

Color: pink; Yield: 81.22%; m.p.: >360°C; M.Wt: 522.25; Elemental analysis for $CoC_{18}H_{24}N_4O_6Cl_2$: found,. C, 39.90; H, 4.66; N, 10.36; Co, 10.99; Cl, 13.50 Calcd, C, 41.40; H, 4.63; N, 10.73; Co, 11.28; Cl, 13.59; Λ_m = 136.20 S cm^2 mol^{-1}; infrared (IR) (KBr, v, cm^{-1}): 3321 m (NH_2), 1666vs (C=O) and 1610vs (C=N) and 582vs, 420vs (M–N).

TABLE 1 The apparatus name and their mode

Type of analysis	Models
Elemental analyses	Perkin Elmer CHN 2400
Molar conductivities	CONSORT K410
FT-IR spectra	FT-IR 460 PLUS (KBr discs) in the range from 4000–400 cm^{-1}
Absorbance measurements	A double beam spectrophotometer (T80 UV/Vis) with wavelength range 190–1100 nm, spectral bandwidth of 2 nm
Magnetic moment	Sherwood scientific magnetic balance using Gouy balance using Hg[Co(SCN)$_4$] as calibrant
^{1}H-NMR spectra	A Varian Mercury VX-300 NMR spectrometer.
TGA-DTG	TGA-50H Shimadzu

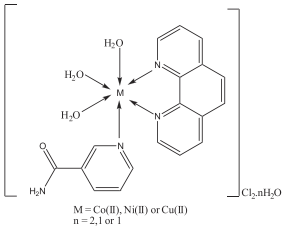

FIGURE 2 The proposed coordination mode of NA, Phen with their complexes

2.2.2 | [Ni (NA)(Phen)$(H_2O)_3$]$Cl_2 \cdot H_2O$

Color: pale blue; Yield: 92.6%; m.p.: 220°C; M.Wt: 503.99; Elemental analysis for $NiC_{18}H_{22}N_4O_5Cl_2$: found, C, 42.36; H, 4.39; N, 10.99; Ni, 11.50; Cl, 13.92. Calcd, C, 42.90; H, 4.40; N, 11.12; Ni, 11.65; Cl, 14.08; Λ_m = 129.2 S cm^2 mol^{-1}; %; IR (KBr, ν, cm^{-1}): 3313 m (NH_2), 1665vs (C=O) and 1604vs (C=N) and 547 ms, 430 s (M–N).

2.2.3 | [cu (NA)(Phen)$(H_2O)_3$]$Cl_2 \cdot H_2O$

Color: cyan; Yield: 84.88%; m.p.: >360°C; M.Wt: 508.84; Elemental analysis for $CuC_{18}H_{22}N_4O_5Cl_2$: found, C 42.42%, H 4.70%, N 10.98%, Cu 12.40%, Cl, 13.87%. Calcd, C, 42.49; H, 4.36; N, 11.01; Cu, 12.49; Cl, 13.95; Λ_m = 142.4 S cm^2 mol^{-1}; IR (KBr, ν, cm^{-1}): 3190 m (NH_2), 1666vs (C=O) and 1614vs (C=N) and 555 m, 422 s (M–N).

2.3 | Theoretical calculations

An endeavor to give a clear insight about the molecular geometry of investigated compounds, geometry optimization, and conformational analysis has been done by means of DFT computations using the GAUSSIAN 98 W set of programs.[10] Using the normal atomic orbital populations, the atomic charges were computed. The high basis set was selected to identify the energies at a very accurate amount.[11]

2.4 | Microbial evaluation

In 250 ml flasks holding 20 ml of working volume of the checked solution, a filter paper disk (5 mm) was moved (100 mg/ml). Both flasks were autoclaved at 121°C for 20 min. Luria Broth (LB) agar media surfaces were inoculated with four investigated bacteria (two Gram-positive bacteria such as *Staphylococcus aureus*, *Bacillus subtilis*, two Gram-negative species *Escherichia coli* and *Salmonella paratyphi*) and two fungi species such as *Aspergillus fumigatus* and *Candida albicans* by diffusion agar technique, then, transferred to a saturated disk with a tested solution in the center of Petri dish (agar plates). All the compounds were put in the inoculated Petri dishes at four equidistant positions at a distance of 2 cm from the middle. The investigated compounds, i.e., ligands and their complexes were dissolved in DMSO (dimethylsulfoxide). Eventually, all these Petri dishes were incubated at 37°C for 24 h and for fungi, 7 days at 30°C, where clear or inhibiting zones were observed around each plate. The tests were run in triplicate, and the results recorded was the average amount.[12] The activity index for the complex was calculated by the formula below[13]:

$$\% \text{ Activity Index} = \frac{\text{Zone of inhibition by test compound (diameter)}}{\text{Zone of inhibition by standard (diameter)}} \times 100$$

2.5 | Assay for DPPH free-radical scavenging potential

The nitrogen centered stable free radical 2,2′-diphenyl-1-picrylhydrazyl (DPPH) has often been used to characterize antioxidants. This is reversibly decreased and gives a high absorption limit at λ 517 nm, which is purple color,[14] to the odd electron in the DPPH free radical. Every assay at various concentrations (100, 200, and 300 μg) of high-performance liquid chromatography (HPLC) methanol was applied to the solution [3.9 ml, 0.004% (w/v)] of DPPH in methanol. The tubes were held for 30 min at room temperature and the absorbance was measured at λ 517 nm. Both experiments were carried out in triplicate and based on average. The percentage of scavenging activity on DPPH expressed as a scavenging activity: SCA% = [(Acontrol − Atest)/Acontrol)] × 100 where Acontrol is the control absorbance (DPPH without sample) and Atest is the sample absorbance (DPPH plus scavenger). The positive controls were tert-butylated hydroxyl quinone (TBHQ) and Butylated hydroxyl anisol (BHA). Both experiments were performed in triplicate, using a mean value.

3 | RESULTS AND DISCUSSION

3.1 | Structural interpretation

Physical analytical data of Phen, NA, and complexes were tabulated in Table S1. The data of the C, H, N, Cl,

and M analysis were found to be in strong alignment with the values determined for the proposed formula $[M\ (NA)(Phen)(H_2O)_3]Cl_2{\cdot}xH_2O$ with 1:1:1 of metal ligands stoichiometry in which both NA and Phen ligands acted as neutral monodentate and bidentate, respectively (Figure 1). The complexes were stable at room temperature in the air and were usually soluble in water, dimethylformamide (DMF), ethanol, and methanol. Molar conductivity values of NA, Phen, and their complexes in DMF with standard reference 1×10^{-3} mol^{-1} solutions at room temperature were established. The results specified that the complexes are electrolytes,[15] and the chloride ions have been detected as counter ions in all complexes.[15] The mass percentage of chloride in the complexes was determined by using two methods.[16,17] The complex structures implied in the elementary investigation are quite in alignment with their proposed formula (Table S1). The measurements of magnetic properties of complexes were performed by the Gouy process in solid state at room temperature. The effective magnetic moments Bohr Magneton (B.M.) of para-complexes were assessed. The Co (II) complex's observed magnetic moment is 4.65 B.M. The higher than spin-only value could be due to metal–metal interaction. The Ni (II) complex magnetic moment magnitude is 3.00 B.M., equivalent to two unpaired d-orbital electrons. The magnetic moment is just similar to the magnitude of rotation. Cu (II) complexes' observed magnetic moments were determined to be 1.95 B.M. The value of this magnetic moment is high with a spin value of just 1.73 B.M. For Cu (II), which means that there is no observable spin–spin coupling between unpaired electrons belonging to various molecules. Consequently, the geometries of Co (II), Ni (II) and Cu (II) complexes were octahedral.[18]

3.2 | IR spectral studies

Here it discusses the fundamental spectral IR bands including corresponding provisional assigns. The Fourier transforms spectra of mixed Phen, NA ligands, and their complexes within the range from 4000–400 cm^{-1} has been mapped out (Figure 3) and assigned to Table S2. Figure 3 represents the proposed structure for all complexes. In order to examine the mode of bonding mixed Phen ligand, NA to metal ion, the IR spectrum of free ligand is contrasted with their metal complexes (Figure 2). The bands for the ν (NH_2) stretches of amide group of NA appear in the range of 3367–3163 cm^{-1}. After chelation, these bands are present within the range of 3321–3197, 3313–3163, and 3367–3190 cm^{-1} for Co (II), Ni (II), and Cu (II) complexes, respectively.[12,19–24] This result confirmed that, in the case of complexes,

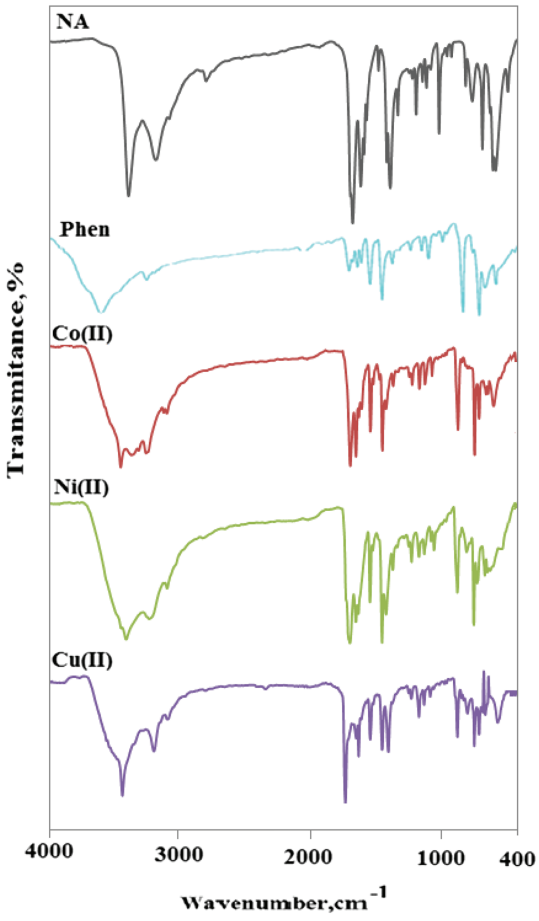

FIGURE 3 Infrared spectra of NA, Phen ligands and their complexes

there is no substantial shift in ν (NH_2) vibrations relative to NA, suggesting non-involvement of the amido group $-NH_2$ in coordination. This observation was related to the hydrogen bonding formation of the amido group between $-NH_2$ and -C=O. The strong absorption band observed around 1668 cm^{-1} are assigned to -C=O stretching vibration of carbonyl of amide group of NA.[19,20] -C=O stretching vibration was observed at 1666, 1665, and 1666 cm^{-1} for Co (II), Ni (II), and Cu (II) complexes, respectively.[12] It can also be argued that NA carbonyl oxygen does not engage in coordination.[23] Whereas vibrations of the NA pyridine ring are observed at 1574 cm^{-1}, complex vibrations are shifted to lower frequencies (1581, 1585, and 1590 cm^{-1}). These changes suggest that coordination occurs between the NA nitrogen atom and metal ions.[23] The bands resulting from the vibrational ν(C=N) mode at 1586 cm^{-1} in Phen were found to be moved to a lower frequency in the metal complexes at 1581–1590 cm^{-1}, suggesting the involvement of pyridine ring nitrogen in the complex formation.[20,21] Chelating by NA and Phen pyridine ring nitrogen atoms is clarified by ν(M-N) bands with differing

intensities at 582 and 420 cm^{-1} for Co (II), 547 and 430 cm^{-1} for Ni (II), and 641 and 547 cm^{-1} for Cu (II) (Table S2), lacking from the NA and Phen spectra. This proves the coordination of the NA and Phen through their pyridyl nitrogen.[12]

3.3 | Electronic spectra and magnetic moments

The absorption spectra of the complexes have been calculated in order to obtain more structural details. UV–Vis spectral data were reported from 200 to 800 nm for the free NA, Phen ligands, and their complexes, as shown in Figure 4 and Table S3, respectively. NA exhibits an absorption band in the ultraviolet regions at 330 nm assigned to π–π* transition and 418 nm assigned to n–π* transition.[25–27] Phen also displays the bands at 217 and 243 nm and at 273 and 350 nm which can be allocated to the π–π* and n–π* transitions, respectively.[25] Upon complexation with metal ions there will be an important change in the electronic properties of the system: (i) A shift to higher or lower in the bands assigned to π–π* and n–π* transition in the complexes.[26,27] (ii) New bands due to charge transfer spectra from ligand to metal (L → M) or metal to ligand (M → L). This transition in visible region due to the ligand-to-metal charge transfer bands (L → M) CT from the electronic lone pairs of adjacent nitrogen or oxygen coordinated to the metal ions.[12,22–28] The electronic spectrum of Co (II) complex showed two d–d transitions bands at 578, 625 nm attributed to $^4T_{1g}(F) \rightarrow {}^4A_{2g}(F)$ and $^4T_{1g}(F) \rightarrow {}^4T_{1g}(P)$ transitions,[12] respectively, in an octahedral architecture. This complex showed the magnetic moment of 4.65 BM. which is close to those reported[12] for Co (II) ions in an octahedral environment. The Ni (II) complex displayed an absorption peak at 562, 670 nm, which can be assigned to $^3A_{2g} \rightarrow {}^3T_{1g}(P)$ and $^3A_{2g} \rightarrow {}^3T_{1g}(F)$ transformation at magnetic moment (3.00 B.M.) and promoting distorted octahedral geometry. The peaks observed at 580 and 620 nm for Cu (II) complex may be assigned to $^2B_{1g} \rightarrow {}^2B_{2g}$ and $^2B_{1g} \rightarrow {}^2E_g$ transitions with the magnetic moment (1.95 B.M.) which dropped for octahedral Cu (II) complexes within the usual range. The values of molar absorption (ε) (Table S3) of the complexes were calculated using 1×10^{-3} M DMSO solution using the relation: $a = \varepsilon bc$, where A = absorption, $c = 1 \times 10^{-3}$ M, b = cell length (1 cm).

3.4 | Nuclear magnetic resonance spectra

In DMSO-d_6 at room temperature, ^{1}H-nuclear magnetic resonance (NMR) spectra of NA, Phen ligands, and their complexes were reported as the solvent, and the details are described in Table S4 and shown in Figure 5. In the

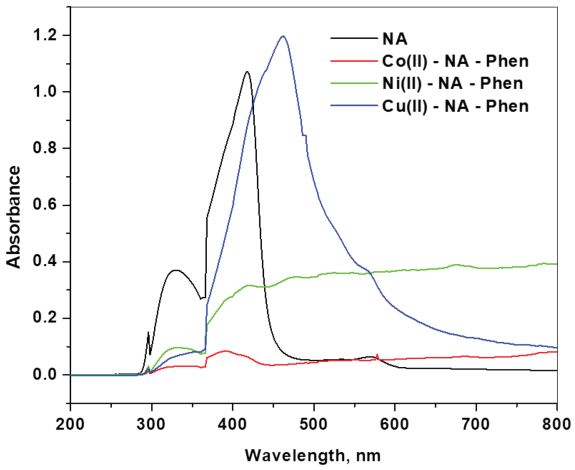

FIGURE 4 Electronic absorption spectral data of NA ligands and their metal complexes

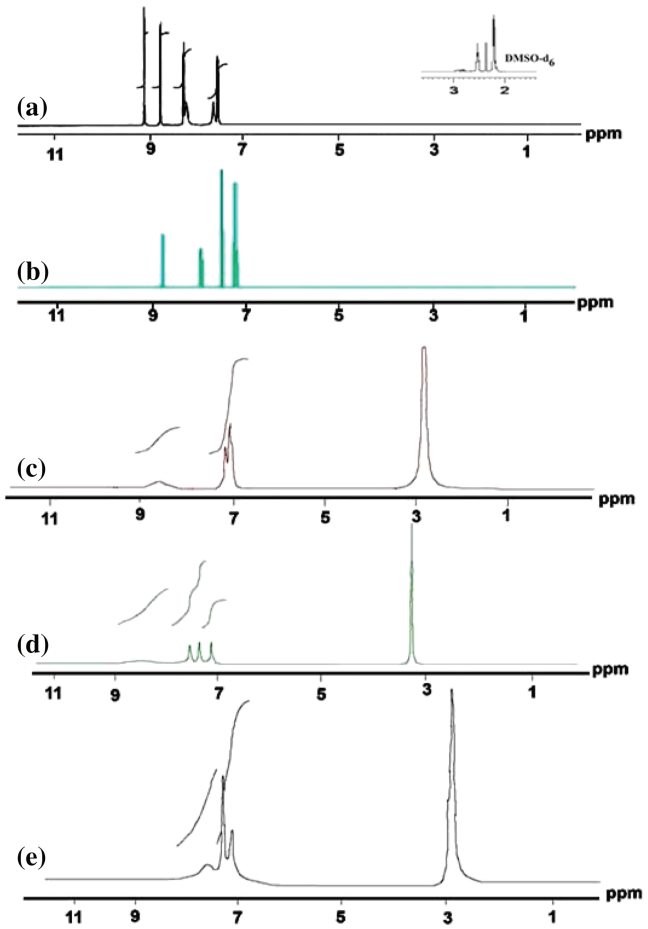

FIGURE 5 ^{1}H-NMR spectra for NA, Phen ligands, and their complexes

DMSO-d_6 solution, the ^{1}H-NMR spectrum of NA ligand is verified. The ^{1}H-NMR spectrum shows a signal assigned to (s,2H,-NH_2) amine protons at δ:7.50 ppm and a multiple signal assigned to aromatic ring protons at δ: 7.57, 8.22, 8.70 ppm. Phen's ^{1}H-NMR spectrum revealed peaks for the protons of the aromatic ring[12,24–28] in the range δ: 7.26, 7.77, 8.11 ppm. The ^{1}H-NMR spectra of NA and Phen ligands have a signal at δ: 9.03 and 8.81 ppm assigned to (s,H,CH=N). The absence of the isomethine (CH=N) proton in the spectra of the complexes suggests the coordination of NA and Phen through its isomethine nitrogen atoms.[9] New signals were detected in the range of 3.37–3.95 ppm in the ^{1}H-NMR spectra of the complexes, owing to the presence of water molecules in the complexes.[28] Thus, the ^{1}H-NMR result supports the geometry assigned.

3.5 | Thermal and thermodynamic parameters analyses

The thermogravimetry (TG) and derivative thermogravimetry (DTG) studies utilized extract details on the thermal stability of the complexes, to assess if the water molecules are within or outside the central metal ion coordination sphere and to propose a general framework for the thermal decomposition of these complexes. The mass loss detected from the TG curves (Figure 6) as seen in Table 2. At a maximum temperature of 276°C, the thermal analysis of NA decomposed with one step with mass loss of 99.58% corresponding to the loss of $3C_2H_2 + N_2O$. Phen decomposition occurs in two phases. The first step of decomposition happens at a mean temperature of 95°C which is followed by a weight loss of 8.02%. The second level of decomposition begins at a height of 278°C with a weight loss of 91.98% leading to a loss of $5C_2H_2 + C_2N_2$.[29] The thermal decay of the Co (II) complex proceeded throughout the temperature range from 40–800°C with four decay phases. The first began at 40–113°C corresponded to lack of two hydrated water molecules (weight loss: 6.79%, calcd. 6.89%). The second step started at 113–387°C and correspond to removal of three coordinated H_2O molecules with mass loss of 10.26% (cal 10.33%). The third stage occurred within 387–477°C with mass loss of 23.44% (cal 23.54%) reflected the loss of chloride anions and partial degradation of the organic ligands. The fourth stages occurred within 477–771°C with mass loss of 35.65% (cal 35.22%)

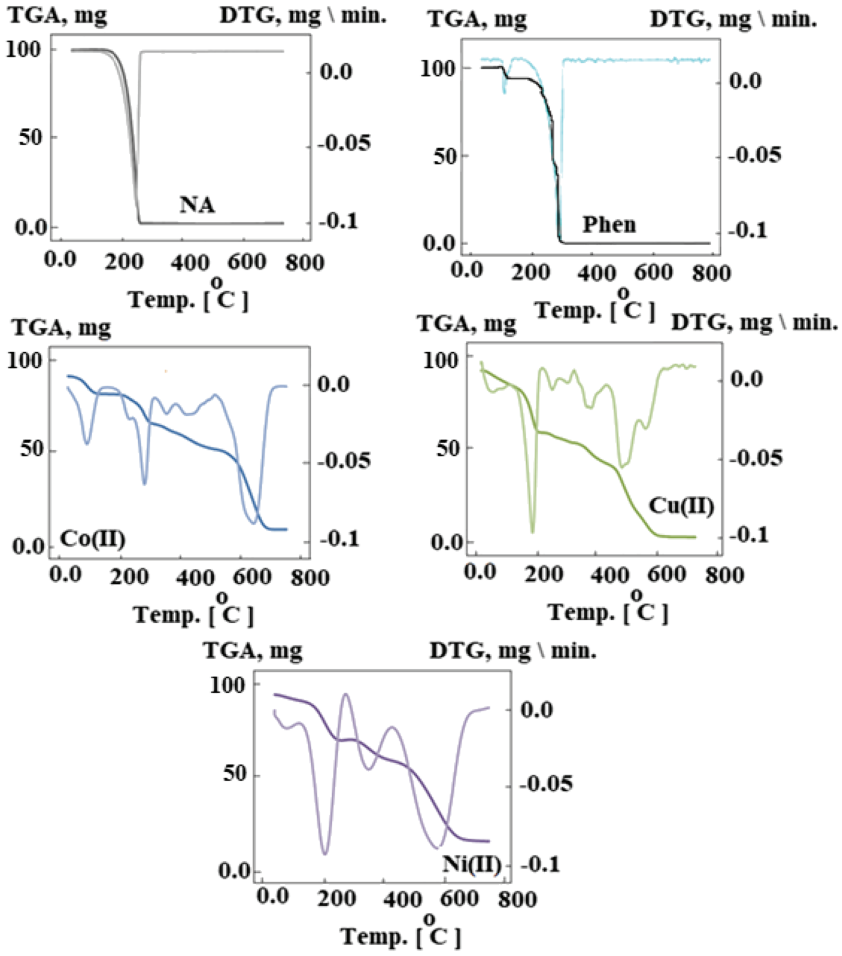

FIGURE 6 TGA and DTG diagrams for the two ligands and their complexes

TABLE 2 The maximum temperature Tmax (°C) and weight loss values of the decomposition stages for NA, Phen, Co (II), Cu (II), and Ni (II) complexes

Compounds	Decomposition	T_{max} (°C)	Weight loss (%)		Lost species
			Calc.	Found	
NA 122.13 ($C_6H_6N_2O$)	First step	263	100	99.58	$3C_2H_2 + N_2O$
					-
	Total loss		100	99.58	
	Residue		-	0.42	
Phen ($C_{12}H_{10}N_2O$)	First step	95	8.07	8.02	$0.5O_2$
	Second step	278	91.93	91.98	$5C_2H_2 + C_2N_2$
	Total loss		100	1z00	
	Residue		-	-	
[Co (NA)(Phen)$(H_2O)_3$]Cl_2·$2H_2O$ 522.25 ($CoC_{18}H_{24}N_4O_6Cl_2$)	First step	113	6.89	6.79	$2H_2O_{hydrated}$
	Second step	256,309,387	10.33	10.26	$3H_2O_{coordinated}$
	Third step	477	23.54	23.44	Loss of chloride anion and partial degradation of the organic ligands ($C_4H_4Cl_2$) assigned to further decomposition of the organic moiety ($C_{14}H_{10}N_4$) leading to the formation of CoO as ultimate product
	Fourth step	671	35.65	35.2	
[Cu (NA)(Phen)$(H_2O)_3$]Cl_2·H_2O 508.84 ($CuC_{18}H_{22}N_4O_5Cl_2$)	First step	96	3.53	3.62	$H_2O_{hydrated}$
	Second step	220,385	24.56	24.22	$3H_2O_{coordinated} + Cl_2$
	Third step	602	56.27	55.97	Definitive degradation of the organic ligand ($C_{18}H_{14}N_4$) leaving CuO as final residue
[Ni (NA)(Phen)$(H_2O)_3$]Cl_2·H_2O 503.99 ($NiC_{18}H_{22}N_4O_5Cl_2$)	First step	101	3.57	3.45	$H_2O_{hydrated}$
	Second step	250, 300, 353, 426	24.80	24.25	$3H_2O_{coordinated} + Cl_2$
	Third step	555	56.81	56.68	Definitive degradation of the organic ligand ($C_{18}H_{14}N_4$) leaving NiO as final residue

and assigned to further decomposition of the organic moiety leading to the formation of CoO as ultimate product. For Cu (II) complex, the first step occurred at 49–112°C, is assigned to the evolution of one hydrated water molecule with a found mass loss of 3.62% (calc. 3.53%). The second one appeared at 112–385°C with found mass loss of 24.22% (calc. 24.56%), representing the loss of three coordinated H_2O molecules and chloride anions. The last step within the temperature range of 385–764°C with weight loss of 55.97% (calc. 56.27%) was assigned to definitive degradation of the organic ligand ($C_{18}H_{14}N_4$) leaving CuO as final residue. For Ni (II) complex, the first step occurred at 51–101°C, is assigned to the evolution of one hydrated water molecules with a found mass loss of 3.45% (calc. 3.57%). The second one appeared at 101–426°C with found mass loss of 24.25% (calc. 24.80%), represent the loss of three coordinated H_2O molecules and chloride anions. The last step within the temperature range of 426–750°C with weight loss of 56.68% (calc. 56.81%) assigned to definitive degradation of the organic ligand ($C_{18}H_{14}N_4$) leaving NiO as final residue. By applying the two methods referred to in the literature[29,30] and outlined in Table 3, the kinetic parameters of degradation steps were calculated and shown in Figure S1. E* values were found to be within the range 56.52–243.57 kJ/mol, with higher values representing the thermal stability of the complexes. The positive values of ΔH* suggest that the composition processes are endothermic[31,32] and the negative values for ΔS* imply that the decomposition reactions take place at a lower rate than the usual ones.[33]

3.6 | Geometrical structure of NA and Phen molecules

The geometrical parameters of the NA ligand were listed in Table S5, the optimized geometry of the two free

TABLE 3 Thermal behavior and Kinetic parameters determined using Coats–Redfern (CR) and Horowitz–Metzger (HM) operated for nicotinamide, phenanthroline, and their metal complexes

				Parameter						
Compounds	Step	T_s (K)	Method	E* (kJ/mol)	A (s^{-1})	ΔS* (kJ/mol. K)	ΔH* (kJ/mol)	ΔG* (kJ/mol)	R[a]	SD[b]
NA	First	536	CR	139.38	2.891×10^{14}	32.56	137.087	128.09	0.99	0.01
			HM	108.97	3.44×10^{20}	148.87	66.74	65.56	0.99	0.005
Phen	Second	551	CR	117.83	2.03×10^{9}	−0.0718	113.25	152.84	0.996	0.12
			HM	146.78	7.97×10^{11}	−0.0222	142.20	154.42	0.998	0.07
[Co (NA)(Phen) $(H_2O)_3$] $Cl_2{\cdot}2H_2O$	Second	660	CR	232.28	7.29×10^{11}	−24.75	226.569	243.57	0.99	0.02
			HM	272.17	1.67×10^{20}	135.28	266.466	173.51	0.99	0.07
[Ni (NA)(Phen) $(H_2O)_3$] $Cl_2{\cdot}H_2O$	Second	523	CR	847.33	1.26×10^{8}	−87.45	828.633	102.53	0.99	0.03
			HM	409.08	1.49×10^{9}	−66.94	414.645	56.52	0.99	0.09
[Cu (NA)(Phen) $(H_2O)_3$] $Cl_2{\cdot}H_2O$	Second	493	CR	110.98	1.16×10^{11}	−30.97	109.066	116.22	0.99	0.13
			HM	571.22	6.199×10^{11}	−17.037	52.0180	59.13	0.99	0.09

[a]Correlation coefficients of the Arrhenius plots.
[b]Standard deviation.

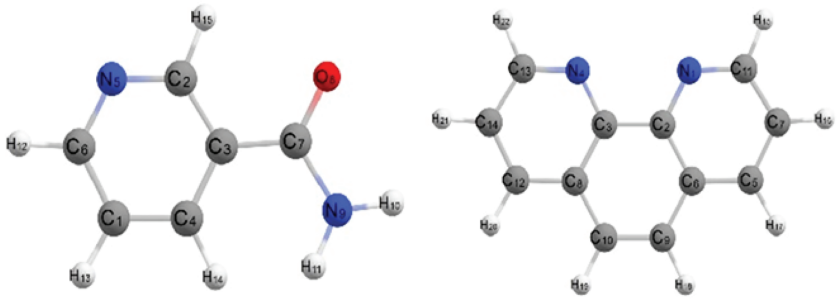

FIGURE 7 The structure of minimized geometrical nicotinamide and phenanthroline ligands by using DFT calculations

ligands, NA and Phen by using DFT calculations view with atomic labeling scheme is shown in Figure 7. The two ligand molecules were completely planar, as reflected by the all torsion angles which varied between 0.00° and 180.00° in case of the two ligands, All bond angles between atoms varied between 117.95° and 123.47°, these values reflects that most atoms has sp^2 hybridization type. There are three donating centers are involved in the NA molecule, from the theoretical investigation we found that the NA molecule can behave as a monodentate ligand through the one nitrogen atom only (N5) of pyridine ring, the agreement between the computed and experimental geometrical parameters is very good. In order to include the optimized geometry of molecules, the mean average difference between the B3LYP/CEP-31G and experimental bond lengths and bond angles is 0.04 Å and 0.00°. In the NA molecule, the average bond distance of -C=N bond ranges between 1.284 and 1.285 Å for C2–N5 and C6–N5, respectively[34] and even the other bond distance of C7-N9 is 1.374 Å,[34] and the bond distance of C7-O8 is 1.209 Å.[35] The distribution of charges on the donating nitrogen and oxygen atoms of the optimized NA molecule geometry and the donating nitrogen atoms of the Phen molecule as seen in Table S5. There is a significant built up of charge density on the two nitrogen atoms (N1 and N4) of Phen ligand, −0.209 and −0.213, respectively and on nitrogen atom (N5) of NA molecule, −0.299. All these values of charge densities enhancing the chelation of NA ligand with metal ion through the one nitrogen atom of the pyridine ring as monodentate and chelation of Phen with metal ion through two nitrogen atoms as bidentate ligand.

3.7 | Complexes geometrical structure

A MO-treatment was applied to elucidate the equilibrium geometry of each species and try to correlate the

geometry of the NA molecule and their Co (II), Ni (II), and Cu (II) complexes to the medical activity, investigate the switch-over process in the configuration of the drug in the time of metal ion–drug bond formation and the charge distribution in studied species. The three metal ions Co (II), Ni (II), and Cu (II) chelated with the two mixed ligands through three coordinated bonds, two of them with N1 and N4 of Phen and the third coordinated bond with N5 of NA ligand. These complexes were treated as octahedral structure, so each one of them tend to complete the six coordination sphere by chelation with three water molecules as reported in experimental part which agree with theoretical investigation.

3.8 | [co (NA)(Phen)$(H_2O)_3]^{2+}$ complex structure

The structure of the atomic numbering scheme complex is seen in Figure 8. In addition to the three water molecules with Co (II), the complex consists of one unit molecule (NA) and one unit molecule (Phen) to complete the octahedral structure. With a slightly periodic octahedral environment around the metal ion, the complex is hexa coordinated. Co (II) is coordinated to form one nitrogen atom (N5) of the NA ligand pyridine group two Phen ligand nitrogen atoms (N1 and N4) and three oxygen atoms of the three water molecules. The bond angle between N1CoN5 is 101.18° and the angle between N4CoN5 is 94.98°, so that the two ligand molecules (NA and Phen) do not lie in the same plane but lie perpendicular to each other. The equatorial plane consists of tetra-donating atoms, one nitrogen atom of Phen (N1), one nitrogen atom of NA (N5) and two oxygen atoms (O6 and O7) of the two water molecules, the bonding angles N1CoO7 and N5CoO6 are 161.86° and 172.92°, indicating that the N1 of Phen and N5 of NA are trans respect to O7 and O6 of water molecules, respectively. Although the axial plane is dominated by the nitrogen atom of Phen (N4) and the oxygen atom of the third water molecule (O8) with a bond angle of 176.31°, from these bond angle values in the equatorial and axial planes it has been confirmed that the two ligands molecules lie perpendicular to each other. The angles between the bonded three water molecules are varied between 81.42° and 85.45°, so all water molecules are lying *cis* respect to others and they are lying *trans* respect to other three bonded toms of the Phen and NA molecules. The bond length between Co-N5 of NA, which is equal 1.918 Å,[36] the bond distances between central Co (II) ion and bonded nitrogen atoms of Phen ligand (N1 and N4) are 1.973[37] and 1.968 Å.[38] The distance between the Co (II) ion and the oxygen atoms of the water molecules (O6, O7 and O8) ranges from 1973 to 1981 Å.[39,40] The angles around Co (II) with surrounding oxygen atoms also range from 79.53° to 176.31°; these values are compatible with those predicted for a slightly normal octahedron. Both bond lengths and bond angles are shown in Table 4. The energy of this complex is −270.775 eV, the heat of formation of this complex is −8715.780 k cal/mol and the dipole value 3.935D is comparatively smaller.

3.9 | The structure of [cu (NA)(Phen) $(H_2O)_3]^{2+}$ complex

Figure S2 demonstrates the optimized geometrical structure of this complex using an atomic numbering schema. With a regular octahedral environment around the metal ion, the complex is hexa coordinated. Two nitrogen atoms (N1 and N4) of Phen, a nitrogen atom (N5) of a NA molecule and three oxygen atoms of the three water molecules are coordinated with Cu (II). The Cu–N5 bond lengths is 1.949 Å,[41] the bond distances between Cu (II) and nitrogen atoms (N1 and N4) of Phen are 2.293 and 2.286 Å,[42] respectively. The bond lengths between Cu (II) and the oxygen atoms O6, O7, and O8 of the three bound water molecules are also 2.244, 2.251, and

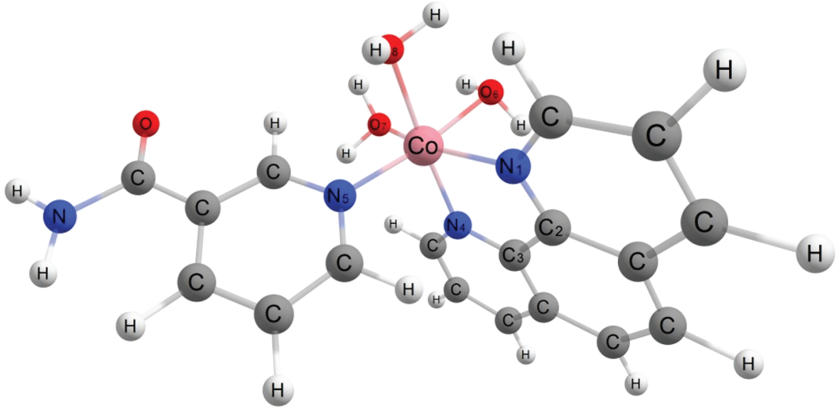

FIGURE 8 Minimized geometrical of [Co (NA)(Phen)$(H_2O)_3]^{2+}$ complex

TABLE 4 The parameters of equilibrium geometric bond lengths (Å), bond angles (°), dihedral angles (°), total energy, heat of formation (k cal/mol), and dipole moment of complexes utilizing DFT measurements

Bond lengths/Å	Co (II)	Cu (II)	Ni (II)
M-N1	1.973	2.293	2.011
M-N4	1.968	2.286	2.016
M-N5	1.918	1.949	2.003
M-O6	1.973	2.244	2.015
M-O7	1.978	2.251	2.018
M-O8	1.981	2.255	2.100
C2-N1	1.264	1.264	1.264
C3-N4	1.265	1.263	1.265
Bond angles/(°)			
N1-M-N4	79.53	79.03	79.63
N1-M-N5	101.18	94.10	95.82
N1-M-O6	81.71	91.41	86.25
N1-M-O7	161.86	179.26	169.89
N1-M-O8	99.51	98.95	97.66
N4-M-N5	94.98	97.43	94.56
N4-M-O6	91.91	84.37	88.44
N4-M-O7	94.41	101.16	101.47
N4-M-O8	176.31	163.32	173.82
N5-M-O6	172.92	174.44	176.61
N5-M-O7	96.35	86.59	94.11
N5-M-O8	88.69	99.23	91.23
O6-M-O7	81.42	87.89	83.75
O6-M-O8	84.43	79.12	85.83
O7-M-O8	85.45	80.67	80.23
Total energy, eV	−270.775	−292.963	−280.923
HF, k cal/mol	−8715.780	−8758.240	−8762.088
Dipole moment, D	3.935	5.099	5.309

2.255 Å,[43] with angles around Cu (II) ranging from 79.03° to 179.26° as seen in Table 4 with surrounding oxygen and nitrogen atoms; these values did not deviate from the normal octahedron. The two ligands molecules are not located in the same plane perpendicular to each other the bond angles N1CuO7 are 179.26° and N5CuO6 is 174.44°, confirming that the two oxygen atoms (O7 and O6) of the two water molecules are trans compared to the NA molecule N1 of Phen and N5, and these four atoms are both located in the equatorial plane. The axial plane is occupied by the nitrogen atom (N4) of Phen and the oxygen atom (O8) of the third water molecule with an angle of 163.32°. Of these values, the two molecules do not occur in the same plane and are perpendicular to each other. The bond angles between water molecules around the Cu (II) ion range from 79.12° to 87.89°, which is consistent with the three bound water molecules lying in *cis* position with respect to each other and the water molecules lying in *trans* position with respect to N1, N4 of Phen and N5 of NA. The energy of this complex is −292.963 eV, this value is smaller than the others such that it is considered more stable than the other two complexes, the dipole value 5.099D is comparatively high and the heat value of the structure is −8758.240 kcal/mol.

3.10 | The structure of [Ni (NA)(Phen) $(H_2O)_3]^{2+}$ complex

The central Ni (II) ion coordination geometry can be envisioned as a curved octahedral configuration as seen in Figure S3, with angles ranging from 79.63° to 176.61° around the Ni (II) ion. The two mixed ligands not lie in the same plane but perpendicular to each other the equatorial plane contains one nitrogen atom, (N1) of Phen, one nitrogen atom, (N5) of NA and two oxygen atoms, (O6 and O7) of the two water molecules. The two remaining coordinated atoms, Phen molecule N4 and oxygen atom O8, are placed in the axial position of the third water molecule. The bond angles N1NiO7 is 169.89°, N5NiO6 is 176.61°, and N4NiO8 is 173.82°, these values proved that the mixed ligands are lying perpendicular to each other and the angle between two to planes is varied between 94.56° and 95.82° for the N4NiN5 and N1NiN5, respectively. The bond angles of the bound water molecules between oxygen atoms range from 80.23° to 85.83°, these values verified that the three water molecules are positioned in cis position with respect to each other and lie trans relative to the other three NA and Phen molecules donating atoms. The bond distances are given in Table 4 between the central metal ion Ni (II) and the surrounding coordinated oxygen and nitrogen atoms. The bond distances between Ni (II) and NA, nitrogen atom (N5) are 2.003,[44] the bond distances between Ni (II) and nitrogen atoms (N1 and N4) of Phen are 2.011 and 2.016 Å,[45] respectively. The bond lengths of the three water molecules between Ni (II) and the oxygen atoms O6, O7 and O8 are also 2.015, 2.018, and 2.100 Å.[46] The energy of this complex is −280.923 eV, highly dipole 5.309D more than others complexes and the value of heat of formation is −8762.088 k cal/mol.

3.11 | Charge distribution analysis

The charge distribution analysis of the designed geometry configuration of NA and their complexes was conducted

on the basis of a natural population analysis (NPA). The selected data is listed in Table 5. The distribution of the charge on the NA molecule suggests the lack of a net negative pole and a net positive pole on the molecule resulting in a weak dipole, μ = 5.458 D. The charge density of the ligand and their complexes seen in Table 6 indicates a comparatively high charge density of the metal ion in the Co (II) complex only the charge accumulated on the Co (II) ion is 0.043, whereas in the case of other complexes the metal ion brings a smaller charge density and the smallest charge is found on the Ni (II) metal ion, 0.011. The negative charge is dispersed to the oxygen atoms of the water molecules and the nitrogen atoms of the two combined ligands, whereas all hydrogen atoms of all complexes display a positive charge. Due to the electronegative character of nitrogen atoms, the carbons immediately attached to Phen's nitrogen atoms (C2 and C3) have more positive values. On the analyzed complexes, the charge density ranges from 0.043 on the Co ion, 0.026 on the Cu ion, and 0.011 on the Ni ion. This study suggests that in each of these complexes, there is an electron back-donation from the metal sites in the MLCT mode to the π* orbitals of the NA and or Phen ligand. This hypothesis is further confirmed by comparing the measured charge density values for donating atoms, pyridine ring nitrogen atoms in NA, Phen ligand, and complexes as seen in Table 5. In determining the position of the dipole moment vector in the complexes, which depends on the centers of negative and positive charges, the distribution of atomic charges is also important.

3.12 | Molecular orbitals and frontier

Molecular orbitals also play an important role in electrical and UV–Vis[47] properties. An electronic device with lower HOMO-LUMO gap values should be more sensitive than one which has a higher energy gap.[48] The energy gap ΔE between the studied complexes differed between 0.149 for Co (II) complex that is more reactive and 0.174 eV for Ni (II) complex that is less reactive, so electron motion between these orbitals could easily occur so that for all studied complexes we find a peak of around 250 nm in the UV–Vis spectra, whereas the energy gap between the two mixed ligands, NA and Phen is 0.373 and 0.2. The energy gap is closely correlated with the performed molecule's reactivity and stabilization, and demonstrates the low kinetic stability and slightly elevated chemical reactivity nature of the molecule. The

TABLE 5 Calculated charges on donating sites and energy values

Parameters	NA	Phen	Co (II)	Cu (II)	Ni (II)
M	-	-	0.043	0.026	0.011
$N1_{phen}$	-	−0.209	−0.113	−0.139	−0.065
$N4_{phen}$	-	−0.213	−0.095	−0.097	−0.139
N5	−0.299	-	−0.084	−0.056	−0.064
O6	-	-	−0.333	−0.316	−0.332
O7	-	-	−0.334	−0.352	−0.318
O8	-	-	−0.312	−0.307	−0.339
HOMO, H	−0.402	−0.396	−0.374	−0.393	−0.375
LUMO, L	−0.029	−0.153	−0.225	−0.225	−0.201
I = -H	0.402	0.396	0.374	0.393	0.375
A = −L	0.029	0.153	0.225	0.225	0.201
ΔE = L-H	0.373	0.243	0.149	0.168	0.174
η = (I-A)/2	0.187	0.122	0.075	0.084	0.087
χ = −(H-L/2)	0.216	0.275	0.299	0.309	0.288
σ = 1/η	5.348	8.197	13.333	11.905	11.494
S = 1/2 η	2.674	4.098	6.667	5.952	5.747
Pi = − χ	−0.216	−0.275	−0.299	−0.309	−0.288
$\omega = (Pi)^2/2\ \eta$	0.125	0.309	0.596	0.568	0.477
$\Delta N_{max} = \chi/\eta$	1.55	2.254	3.987	3.679	3.310

Note: HOMO, LUMO, Energy gap ΔE/eV, hardness (η), global softness (S), electro negativity (χ), absolute softness (σ), chemical potential (Pi), global electrophilicity (ω), and additional electronic charge (ΔNmax) of the free ligands NA, Phen, and their studied complexes by using DFT calculations.

TABLE 6 The inhibition diameter zone values (mm) for NA, Phen, and their complexes

Compounds	Microbial species					
	Bacteria				fungi	
	E. coli	*Salmonella*	*S. aureus*	*B. subtilis*	*A. fumigatus*	*C. albicans*
NA	6 ± 0.34	8 ± 0.11	5 ± 0.12	8 ± 0.4	-	-
Co (II)- NA- phen	15^{***} ± 0.83	15^{***} ± 1.3	18^{****} ± 2.2	18^{***} ± 0.23	15^{****} ± 0.03	12^{***} ± 0.01
Ni (II)- NA- phen	14^{***} ± 0.8	8^{*} ± 0.8	12^{***} ± 0.12	12^{**} ± 1.1	-	17^{****} ± 0.02
Cu (II)- NA- phen	11^{**} ± 1.1	12^{***} ± 1.1	9^{*} ± 2.2	10^{**} ± 0.6	11^{***} ± 0.96	-
Standard Nystain antifungal agent	-	-	-	-	11 ± 1.2	-
Amphotericin B Antifungal agent	-	-	-	-	-	19 ± 0.11
Amoxycillin/Clavulanic antibacterial agent	12 ± 1.2	11 ± 0.96	15 ± 1.1	-	-	-

Note: Values were recorded as the mean inhibition percentage of microbial growth (three replicates) ± SDs. Statistical values were significantly different according to Student's t-test (paired) at $P < 0.05$.

$^{*}P < 0.05$ (not significant).

$^{**}P > 0.05$ (significant).

$^{***}P > 0.01$ (highly significant).

$^{****}P > 0.001$ (very highly significant).

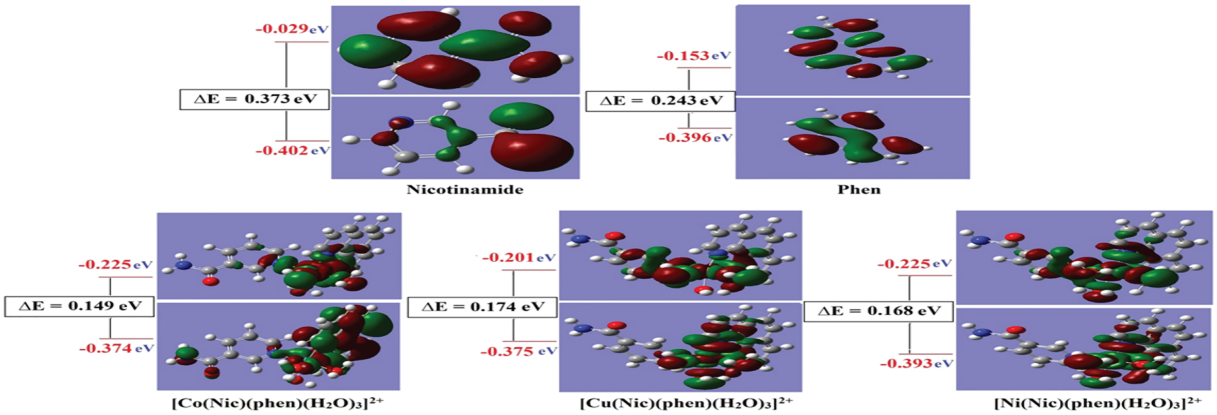

FIGURE 9 Molecular orbital surfaces and energy levels of nicotinamide, Phen and their complexes, (a) $[Co\ (NA)(Phen)(H_2O)_3]^{2+}$, (b) $[Cu\ (NA)(Phen)(H_2O)_3]^{2+}$, and (c) $[Ni\ (NA)(Phen)(H_2O)_3]^{2+}$ by using DFT calculations

neighboring orbitals, on the other hand, are always closely spaced in the frontier zone. The nodal features of the molecular orbitals in the complexes described in Figure 9 is demonstrative and suggests orbital delocalization, high orbital overlap, and low nodal plane numbers. Those features contribute to UV–Vis. The spectrum is distinguished by the presence of phases of charge transfer: low energy and high intensity bands. A different degree of localization on the different fragments of the complexes is seen by the different MOs, and the above rationalization is true for MO analysis of all the complexes studied. The energy difference between HOMO and LUMO (energy gap, ΔE) varied according to the form of metal ion, as seen in Table 5, for all complexes studied. Many of the complexes tested have a smaller energy gap than free ligands, so these complexes are more receptive than free ligands. Figure 9, demonstrates HOMO and LUMO's isodensity surface plots for free ligand and their complexes. For the NA ligand, with the exception of one carbon atom involved only in the pyridine ring, the electron density of HOMO is delocalized and distributed over all fragments of the NA ligand, whereas the electron density of LUMO is delocalized and spread over all atoms in the NA molecule. The electron density of HOMO and LUMO in Phen ligand is delocalized and distributed over all Phen molecule

fragments except one carbon atom only. The hardness (a is defined as (a = (I-A)/2) where I is the energy of ionization and A is the affinity of electrons. The (I-A), on the other hand, refers to the distance between HOMO and LUMO. Therefore it is possible to measure the hardness of the ligands and their complexes as (η = [EHOMO-ELUMO]/2). The HOMO-LUMO gap is large in hard molecules, and soft molecules have a lower HOMO-LUMO gap.[48] The values of η and ΔE (HOMO-LUMO) are given in Table 5. It is clear from the table that both complexes range from 0.087 for Ni (II) complex to 0.075 for Co (II) complex, whereas η for NA and Phen ligands differ from 0.087 for Ni (II) complex to 0.075 for Co (II) complex. As shown by the ΔE of complexes, the electronic transfer within complexes is simple and these energy gap values for complexes are in line with the standards for stable complexes. Based on the energy values of HOMO and LUMO, certain quantum chemical parameters are measured as global softness (S), electronegativity (χ), absolute softness (σ), chemical potential (Pi), global electrophilicity (ω), and additional electronic charge (ΔNmax) of the free ligands and tested complexes. Accordingly to (σ = 13.333 eV), the Co (II) complex is absolute soft, whereas the Ni (II) complex is treated as a hard complex (σ = 11.494 eV). In comparison to the free ligands, the (σ) of NA and Phen are 5.348 and 8.197 eV respectively, all studied complexes known as soft complexes.

3.13 | Excited state

Using the G03W application, the TD-DFT at the B3LYP level proved to provide a precise UV–Vis explanation.[49–51] Spectra The functional reaction principle of time-dependent density (TD-DFT) has recently been reformulated[51] to measure discrete transition energies and strengths of oscillators and has been generalized to a variety of different atoms and molecules.[52] In the measurement of excitation energies, Bauernschmitt and Ahlrichs[53] used hybrid functionals proposed. Typically, these hybrid approaches represent a major advancement over traditional methods based on Hatree- Fock (HF). The optimized geometry was determined in this work and was used in all subsequent calculations; the wave functions of SCF MOs were studied directly. The measured wave functions of the various MOs represent and signify the fraction of the complex's different fragments adding to the different states' overall wave functions. The findings suggest that the spectrum of electron delocalization in the various molecular orbitals is present. The electronic transition could be described as a mixed $n \rightarrow \pi^*$ and $\pi \rightarrow \pi^*$ transitions. Table 5 lists the energies of HOMO and LUMO states for free ligands and all the complexes tested. The HOMO will behave in the reaction profile as an electron donor and the LUMO as the electron acceptor. The electron density of HOMO is found in the Co (II) complex specifically on all Phen ligand atoms, metal ions with surrounding donating atoms and carbonyl groups of NA molecules, whereas LUMO is located only on the metal ions with surrounding donating atoms. The electron density of HOMO is located predominantly on the central metal ion with the surrounding donating atoms specifically two nitrogen atoms of Phen ligand in Cu (II) and Ni (II) complexes, but the LUMO of these complexes are located on the metal ion with the surrounding donating atoms Phen and NA ligands, so the electronic transformation may be defined as transitions of mixed $n \rightarrow \pi^*$ and $\pi \rightarrow \pi^*$.The striking feature of the studied Cu (II) and Ni (II) complexes are that the HOMO and LUMO orbitals are focused on the Phen ligand and central metal ion only, which gives arise to the possibility of MLCT from metal ion to either Phen(π^*).[54]

4 | BIOLOGICAL APPLICATIONS

4.1 | In vitro antibacterial and antifungal activities

In vitro antibacterial and antifungal activities of the two ligands NA, Phen as well as their metal complexes (Co (II), Ni (II), and Cu (II)), were tested against *S. aureus*, *B. subtilis* as gram- positive bacteria, *E. coli* and *Salmonella paratyphi* as gram-negative bacteria and *A. fumigatus* and *C. albicans* as fungi. According to the data depicted in Figure 10 and tabulated in Table 6, the following results are summarize as follow: All of the tested compounds are found to have remarkable antibacterial and satisfied antifungal activities. The active sequence of the ligand and their tested complexes against *S. aureus* follows the trend: Co (II) > Ni (II) > Cu (II) > NA, *B. subtilis* Co (II) > Ni (II) > Cu (II) > NA, *E. coli* Co (II) > Ni (II) > Cu (II) > NA. *Salmonella paratyphi* Co (II) > Cu (II) > Ni (II) > NA, *A. fumigatus* Co (II) > Cu (II) > Ni (II) = NA, *C. albicans* Ni (II) > Co (II) > Cu (II) = NA. It is found that, Co (II) complex has the highest toxicity against gram-positive, gram-negative bacteria and fungi (*A. fumigatus*). Moreover, it is found that all tested complexes are more toxic against both gram-positive, gram-negative bacteria and fungi than that of the free ligand. This would suggest that, chelation/complexation could enhance the lipophilic character of the central metal atom which explained by Tweedy's chelation theory.[54] It is suspected that other factors such as liposolubility, dipole moment, conductivity influenced by

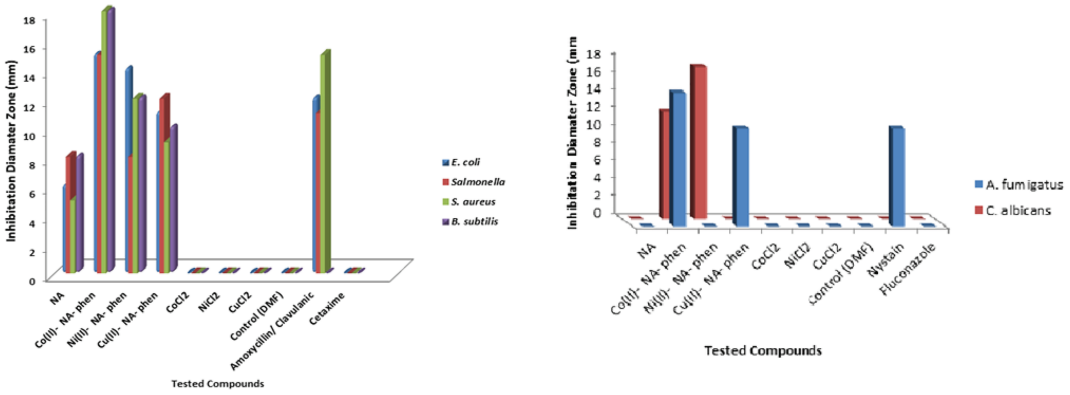

FIGURE 10 Antibacterial and antifungal activity for the ligand and their metal complexes

metal ion, geometry, number and type of metal ions and counter ions may be possible reasons for their remarkable antibacterial and antifungal activities.[20]

4.2 | Antioxidant activity

The method of scavenging DPPH free radicals has been used to assess the antioxidant activity of the ligand and isolated solid complexes.[55] The results of the inhibition ratio for DPPH was registered in Table S6. The results is compared to those of traditional antioxidants. At three concentrations (100, 200, and 300 μg ml^{-1}), the radical scavenging activity percentage of the synthesized complexes was reached. The scavenging activity of DPPH was represented as IC_{50}, an important concentration at which antioxidant activities were measured at 50% of the repressed radicals. A lower IC_{50} value was elucidated by more antioxidant activity. Efficient antioxidant function usually indicates that IC_{50} values are smaller than 10 mg/ml. Figure 11 indicates that at varying concentrations, all the studied compounds displayed very strong radical scavenging behaviors. As opposed to the positive norm and all measured complexes, the ligand (IC_{50} = 0.514 μg ml^{-1}) has the lowest scavenging efficiency. The order of IC_{50} values of ligand and their metal complexes was as follows: Ni (II) > Co (II) > Cu (II) > Ligand (NA). The free radical scavenging activity of the compounds depends on the structural factors such as type and geometry of metal ions.

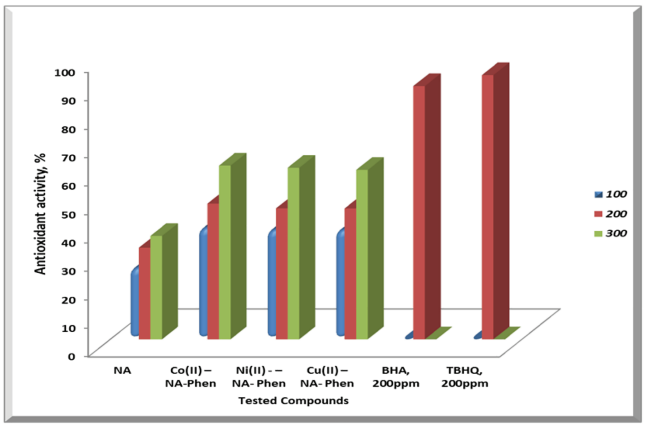

FIGURE 11 Antioxidant activity of ligand and their complexes as determined by DPPH

5 | CONCLUSIONS

New mixed ligand metal complexes were synthesized and characterized. Mononuclear complexes were obtained from the chelation of NA and Phen with Co (II), Ni (II), and Cu (II). Characterization and structure clarification of the metal complexes was carried out by means of different analytical and spectroscopic tools. The results showed that NA and Phen reacted with metal ions as unidentate and bidentate ligands via one and two pyridyl nitrogen atoms of NA and Phen, respectively. The coordination number of all complexes is 6. The results of this investigation support the suggested octahedral structure of the metal complexes and form a favorable molecular arrangement. Kinetic parameters of thermal decomposition stages have been evaluated using Coats–Redfern and Horowitz–Metzger equations. The activation energy (E*) values were found in the range 108.97–847.33 kJ/mol. The proposed structure of the prepared complexes was geometrically optimized and the molecular parameter of NA and its metal complexes has been calculated. The calculated energy gap (ΔE/eV) values were found in the range from 0.149 to 0.373. The antimicrobial efficiencies of the compounds have been checked against various kinds of bacteria and fungi strains. The obtained results showed that the tested compounds have low to moderate antimicrobial efficacy towards the examined

microorganisms in comparison to the well-known standard drugs. It is found that, Co (II) complex has the highest toxicity against gram-positive, gram-negative bacteria and fungi (*A. fumigatus*). The antioxidant activity of the chelates has been tested. The overall order of the observed IC_{50} values of the complexes was Ni (II) > Co (II) > Cu (II).

ACKNOWLEDGMENTS

The authors gratefully acknowledge Zagazig University, Egypt, and University of Bisha, Saudi Arabia, for the support of this research work.

AUTHOR CONTRIBUTIONS

walaa el-shwiniy: Project administration; software; supervision; visualization. **M. G. Abd Elwahed:** Supervision; validation; visualization. **Reham Saeed:** Conceptualization; data curation; formal analysis; funding acquisition; investigation; methodology; resources. **Wael A. Zordok:** Conceptualization; data curation; software; validation. **Sameh El-Desoky:** Funding acquisition; investigation; supervision.

DATA AVAILABILITY STATEMENT

The data that support the findings of this study are available from the corresponding author upon reasonable request.

CONFLICT OF INTEREST

This research holds no conflict of interest and is not funded through any source.

ORCID

Walaa H. El-Shwiniy https://orcid.org/0000-0002-7577-8090
Mohamed G. Abd Elwahed https://orcid.org/0000-0002-1514-8900
Reham M. Saeed https://orcid.org/0000-0001-8309-904X
Wael A. Zordok https://orcid.org/0000-0002-2919-5927
Sameh I. El-Desoky https://orcid.org/0000-0002-5220-0018

REFERENCES

[1] A. A. Rasool, A. A. Hussain, L. W. Dittern, *J. Pharm. Sci.* **1991**, *80*, 387.
[2] G. Turhan-Zitouni, M. Sıvacı, F. S. Kılıç, K. Erol, *Eur. J. Med. Chem.* **2001**, *36*, 685.
[3] M. P. Evstigneev, V. P. Evstigneev, A. A. Hernandez Santiago, D. B. Davies, *Eur. J. Pharm. Sci.* **2006**, *28*, 59.
[4] A. S. Mildvan, M. Cohn, *J. Bio. Chem.* **1966**, *241*, 1178.
[5] R. E. Coffman, D. O. Kildsig, *J. Pharm. Sci.* **1996**, *85*, 951.
[6] L. Y. Lim, M. L. Go, *Eur. J. Pharm. Sci.* **2000**, *10*, 17.
[7] Ö. Altun, M. Şuözer, *J. Mol. Struct.* **2017**, *1149*, 307.
[8] S. M. Abd El-Hamid, S. A. Sadeek, W. A. Zordok, W. H. El-Shwiniy, *J. Mol. Struct.* **2019**, *1176*, 422.
[9] S. A. Sadeek, S. M. Abd El-Hamid, W. H. El-Shwiniy, *Res. Chem. Intermed.* **2016**, *42*, 3183.
[10] M. J. Frisch, G. W. Trucks, H. B. Schlegel, G. E. Scuseria, M. A. Robb, J. R. Cheeseman, V. G. Zakrzewski, J. A. Montgomery Jr, R. E. Stratmann, J. C. Burant, S. Dapprich, J. M. Millam, A. D. Daniels, K. N. Kudin, M. C. Strain, O. Farkas, J. Tomasi, V. Barone, M. Cossi, R.. Cammi, B. Mennucci, C. Pomelli, C. Adamo, S. Clifford, J. Ochterski, G A. Petersson, P. Y. Ayala, Q. Cui, K. Morokuma, K. D. MalickMalick, A. D. Rabuck, K. Raghavachari, J. B. Foresman, J. Cioslowski, J. V. Ortiz, B. B. Stefanov, G. Liu, A Liashenko, P. Piskorz, I. Komaromi, R. Gomperts, R. L. Martin, D. J. Fox, T. Keith, M. A. Al-Laham, C. Y. Peng, A. Nanayakkara, C. Gonzalez, M. Challacombe, P. M. W. Gill, B. Johnson, W. Chen, M. W. WongWong, J. L. Andres, C. Gonzalez, M. Head-Gor-don, E. S. Replogle, J. A. Pople, *Gaussian98*, Revision A.6, Inc., Pittsburgh PA **1998**.
[11] W. J. Stevens, M. Krauss, H. Bosch, P. G. Jasien, *Can. J. Chem.* **1992**, *70*, 612.
[12] W. H. El-Shwiniy, W. S. Shehab, W. A. Zordok, *J. Mol. Struct.* **2020**, *1199*, 126993.
[13] T. A. Yousef, O. A. El-Gammal, S. F. Ahmed, G. M. Abu El-Reash, *Spectrochim. Acta a* **2015**, *135*, 690.
[14] M. S. Blois, *Nature* **1958**, *181*, 1199.
[15] W. J. Geary, *Coord. Chem. Rev.* **1971**, *7*, 81.
[16] A. I. Vogel, *Qualitative Inorganic Analysis*, 6th ed., revised by G. Svehla, Wiley, New York **1987** 174.
[17] V. Alexeyev, *Quantitative Analysis*, 2nd ed., MIR Publishers, Moscow **1969** 519.
[18] (a)L.-N. Zhu, M. Liang, Q.-L. Wang, W.-Z. Wang, D.-Z. Liao, Z.-H. Jiang, S.-P. Yan, P. Cheng, *J. Mol. Struct.* **2003**, *657*, 157. (b)K. Burger, T. Tan, D. W. Allen, *Coordination Chemistry: Experimental Method*, Butterworth, London **1973**.
[19] F. E. Özbek, M. Sertçelik, M. Yüksek, H. Necefoğlu, R. Ç. Ç. Gamze, Y. Nayir, T. Hökelek, *J. Mol. Struct.* **2017**, *1150*, 112.
[20] K. Nakamoto, *Infrared and Raman Spectra of Inorganic and Coordination Compounds*, Wiley, New York **1986**.
[21] D. A. Köse, H. Necefoğlu, O. Şahin, O. Büyükgüngör, *J. Chem. Crystallogr.* **2011**, *41*, 297.
[22] D. A. Köse, A. N. Ay, O. Şahin, O. Büyükgüngör, *J. Iran. Chem. Soc.* **2012**, *9*, 591.
[23] M. A. Gamil, S. A. Sadeek, W. A. Zordok, W. H. Elshwiniy, *J. Mol. Struct.* **2020**, *1209*, 127941.
[24] W. H. El-Shwiniy, W. A. Zordok, *Spectrochim. Acta a* **2018**, *199*, 290.
[25] S. A. Sadeek, S. M. AbdEl-Hamid, *J. Mol. Struct.* **2016**, 1122, *1122*, 175.
[26] E. Vinuelas-Zah, M. A. Maldonado-Rogado, F. Luna-Giles, F. J. Barros-Garc, *Polyhedron* **2008**, *27*, 879.
[27] O. F. Ozturk, M. Sekerci, E. Ozdemir, *Russ. J. Coord. Chem.* **2005**, *31*, 651.
[28] W. H. El-Shwiniy, L. M. Abbass, S. A. Sadeek, W. A. Zordok, *Russ. J. Gen. Chem.* **2020**, *90*, 483.
[29] A. W. Coats, J. P. Redfern, *Nature* **1964**, *201*, 68.
[30] S. A. Sadeek, S. M. Abd El-Hamid, *J. Therm. Anal. Calorim.* **2016**, *124*, 547.

[31] M. M. Omar, *J. Therm. Anal. Calorim.* **2009**, *96*, 607.
[32] A. Rotaru, M. Gosa, P. Rotaru, *J. Therm. Anal. Calorim.* **2008**, *94*, 367.
[33] J. W. Moore, R. G. Pearson, *Kinetics and Mechanism*, John Wiley, New York **1981**.
[34] A. I. Daud, W. M. Khairul, H. Mohamed Zuki, K. KuBulat, J. Sulfur, *Chem* **2014**, *35*, 691.
[35] A. Saeed, S. Ashraf, U. Flörke, Z. Y. D. Espinoza, M. F. Erben, H. Pérez, *J. Mol. Struct.* **2016**, *1111*, 76.
[36] K. K. Gangu, S. Maddila, S. B. Mukkamala, S. B. Jonnalagadda, *J. Mol. Struct.* **2017**, *1143*, 153.
[37] T. R. Todorovic, A. Bacchi, D. M. Sladic, N. M. Todorovic, T. T. Boz˘ic, D. D. Radanovic, N. R. Filipovic, G. Pelizzi, K. K. Andelkovic, *Inorg. Chim. Acta* **2009**, *362*, 3813.
[38] A. Bailey, W. P. Griffith, D. W. C. Leung, A. J. P. White, D. J. Williams, *Polyhedron* **2004**, *23*, 2631.
[39] A. Di Santo, D. M. Gil, F. Pomiro, O. E. Piro, G. A. Echeverria, M. Arena, C. Luciardi, R. E. Carbonio, A. B. Altabef, *Inorg. Chim. Acta* **2015**, *436*, 16.
[40] Y. F. Yue, W. Sun, E. Q. Gao, C. J. Fang, S. Xu, C. H. Yan, *Inorg. Chim. Acta* **2007**, *360*, 1466.
[41] E. H. Oliveira, G. E. A. Medeiros, C. Peppe, M. A. Brown, D. G. Tuck, *Can. J. Chem.* **1997**, *75*, 499.
[42] M. R. Moya-Hernández, A. Mederos, S. Domínguez, A. Orlandini, C. A. Ghilardi, F. Cecconi, E. González-Vergara, A. Rojas-Hernández, *J. Inorg. Biochem.* **2003**, *95*, 131.
[43] H. H. Repich, S. I. Orysyk, V. V. Orysyk, Y. L. Zborovskii, A. K. Melnyk, V. V. Trachevskyi, V. I. Pekhnyo, M. V. Vovk, *J. Mol. Struct.* **2017**, *1146*, 222.
[44] G. Tamasi, *Open Crystallogr. J.* **2010**, *3*, 41.
[45] O. Z. Yesilel, M. S. Soylu, H. Olmez, O. Buyukgungor, *Polyhedron* **2006**, *25*, 2985.
[46] M. Guricová, M. Pizl, Z. Smékal, L. Nádherny, J. Cejka, V. Eigner, I. Hoskovcová, *Inorg. Chim. Acta* **2018**, *477*, 248.
[47] I. Fleming, *Frontier Orbitals and Organic Chemical Reactions*, Wiley, London **1976**.
[48] R. Kurtaran, S. Odabasoglu, A. Azizoglu, H. Kara, O. Atakol, *Polyhedron* **2007**, *26*, 5069.
[49] K. Krogmann, Z. Anorg, *Allg. Chem.* **1966**, *346*, 188.
[50] I. Ciofini, P. P. Laine, F. Bedioui, *C. Admo. J. Am. Chem. Soc.* **2004**, *126*, 10763.
[51] I. Ciofini, C. Daul, C. J. Adamo, *J. Phys. Chem. A* **2003**, *107*, 11182.
[52] F. M. Casida, in *Recent Advances in Density Functional Methods, Part 1*, (Ed: D. P. Chong), World Scientific, Singapore **1995**.
[53] R. Bauernschmitt, R. Ahlrichs, *Chem. Phys. Lett.* **1996**, *256*, 454.
[54] W. H. El-Shwiniy, A. G. Ibrahium, S. A. Sadeek, W. A. Zordok, *Appl. Organometal. Chem* **2021**, *35*, e6174.
[55] A. T. Bilgicli, Y. Tekin, E. H. Alici, M. N. Yaraşir, G. Arabaci, M. Kandaz, *J. Coord. Chem.* **2015**, *68*, 4102.

SUPPORTING INFORMATION

Additional supporting information may be found online in the Supporting Information section at the end of this article.

How to cite this article: El-Shwiniy WH, Elwahed MGA, Saeed RM, Zordok WA, El-Desoky SI. Structural elucidation, molecular modeling, and biological and antioxidant studies of phenanthroline/nicotinamide metals complexes. *Appl Organomet Chem*. 2021;35:e6231. https://doi.org/10.1002/aoc.6231